Understanding Controls on Historical River Discharge in the World's Largest Drainage Basins

Christopher Potter*

NASA Ames Research Center, Moffett Field, California

Pusheng Zhang

University of Minnesota, Minneapolis, Minnesota

Steven Klooster and Vanessa Genovese

California State University, Monterey Bay, Seaside, California

Shashi Shekhar and Vipin Kumar

University of Minnesota, Minneapolis, Minnesota

Received 2 July 2003; accepted 29 October 2003

ABSTRACT: Long-term (20 yr) river discharge records from 30 of the world's largest river basins have been used to characterize surface hydrologic flows in relation to net precipitation inputs, ocean climate teleconnections, and human land/water use patterns. This groundwork study is presented as a precedent to distributed simulation modeling of surface hydrologic flows in large river basins. Correlation analysis is used as a screening method to classify

* Corresponding author address: Dr. Christopher Potter, NASA Ames Research Center, Moffett Field, CA 94035.

E-mail address: cpotter@mail.arc.nasa.gov

river basins into categories based on major controls on discharge, for example, climate, land use, and dams. Comparisons of paired station records at upstream and downstream discharge locations within each major river basin suggest that the discharge signals represented in upstream discharge records are sustained in the downstream station records for nearly two-thirds of the drainage basins selected. River basins that showed the strongest localized climate control over historical discharge records, in terms of correlations with net basinwide precipitation rates, are located mainly in the seasonally warm temperate and tropical latitude zones, as opposed to river basins located mainly in the higher latitude zones (above 45°N). Ocean climate indices such as the Niño1+2 and Niño3+4 correlate highly with historical interannual patterns in monthly river discharge for only four of the selected discharge station records, namely, on the Amazon, Congo (Zaire), Columbia, and Colorado (Arizona) Rivers. Historical patterns of cropland development and irrigated areas may explain the weak climate correlations with interannual patterns in monthly river discharge rates for at least one-third of the major river drainages selected from the historical discharge dataset.

This paper is part of a special theme issue on land use and ecosystems.

KEYWORDS: River discharge, Land use, Climate

1. Introduction

Large rivers integrate the constituents and characteristics of the landscape through which they flow. Consequently, river discharge represents a valuable historical record of hydrologic patterns over complex drainage basins, and therefore has a particularly important role to play in understanding climatic and anthropogenic effects on terrestrial ecosystems at continental and global scales (Vörösmarty and Sahagian, 2000).

River flow has important implications for physics in the Earth's oceans, including effects on circulation and salinity near the mouth of large rivers. For example, the thermohaline circulation is closely linked to the freshwater balance of the Arctic Ocean basin (Driscoll and Haug, 1998). In semiclosed inland seas, such as the Mediterranean, circulation is strongly influenced by riverine inputs of freshwater. River discharge plays a key role in transport of dissolved and particulate materials within and from all the continents (Ludwig and Probst, 1998) and is a major control on the chemistry and biology of the world's major estuaries and coastal fisheries (Caddy and Bakun, 1994).

Rates of river discharge are controlled from one month to the next by several interrelated physical, biological, and anthropogenic factors that may be coupled on scales from regional to global. In a worldwide study of discharge patterns by Dettinger and Diaz (Dettinger and Diaz, 2000), monthly river flow records from over 1000 station sites were analyzed to characterize geographic differences in the seasonality and year-to-year variability of river flow. The river discharge sites were selected to be "reasonably free from human-induced discontinuities." Results from this analysis implied that seasonality in river discharge rates varies regionally, depending on the timing of maximum precipitation (PREC), potential evapotranspiration (PET), and snowmelt. For example, river discharge rates in eastern and southern South America, the southwestern United States, northern Europe, and

Australia correlate well with variations in El Niño–Southern Oscillation (ENSO) climate indices (CIs). Other variations in river discharge records from the eastern United States, Europe, and tropical South America and northern Africa reflect the North Atlantic Oscillation (NAO). Potter et al. (Potter et al., 2003) have reviewed evidence that NAO influences the climate and vegetation dynamics of tropical South America.

Oceanic climate is not the only factor potentially influencing discharge rates within large drainage basins. Rivers represent the primary source of freshwater for human use, including potable water, crop irrigation, hydropower, transportation, and waste processing. Consequently, human-induced changes in river systems cannot be ignored in understanding seasonal and long-term discharge patterns of discharge flows. For example, Coe (Coe, 2000) reported that including man-made dams and reservoirs on some large rivers improves the agreement of the simulated mean monthly discharge with observations, by reducing the amplitude of the simulated seasonal cycle.

The general question we address in this study is, "What are the major controllers of surface water discharge rates within the world's largest river basins?" Our objectives are to understand the changes in controllers of river discharge processes and patterns as water flows from the upstream source locations to downstream locations near the river's mouth. Our data analysis approach using discharge records together with climate, land management, and basinscale geographic relationships is presented as a groundwork study to precede distributed simulation modeling of surface hydrologic flows in large river basins. Correlation analysis is used as a screening method to classify river basins into categories based on major controls on discharge, for example, climate, land use, and dams.

Specific research questions include

- To what extent do net monthly precipitation rates (PREC − PET) along a river drainage system explain the historical (1958–98) interannual pattern and intrabasin (upstream versus downstream) differences in monthly river discharge rates?
- To what extent do CIs correlate with monthly PREC − PET rates along a river drainage system to explain the historical (1958–98) interannual pattern and intrabasin differences in monthly river discharge rates?
- To what extent does water use associated with past agricultural (cropland) development along a river drainage system explain the historical (1958–98) interannual pattern and intrabasin differences in monthly river discharge rates?
- To what extent does water use associated with current land cover and land use along a river drainage system explain the contemporary intrabasin differences in monthly river discharge rates?

2. Review of previous regional studies of historical river discharge

There have been several previous studies of the potential impacts of CIs on river discharge rates in the world's large hydrologic drainage basins. Major results from these studies are summarized below according to continent.

2.1. North America

Barros and Evans (Barros and Evans, 1997) reported an increase in the number of large flood events in the upper Mississippi River basin from 1982 to 1994 as consistent with the strengthening of ENSO activity during this period. Foreman et al. (Foreman et al., 2001) reported that flow rates were lower and water temperatures were higher on the lower Fraser River during the summers following El Niño events. In a trend analysis of twentieth-century discharge rates for nine large river basins, Milly and Dunne (Milly and Dunne, 1998) found that in North America only trends for the St. Lawrence River (+30%) were significant and could not be related to any known anthropogenic effects.

In the Columbia River basin, there is a tendency for decreased snowmelt discharge during El Niño years and increased melt discharge during La Niña years (Clark et al., 2001; Hamlet and Lettenmaier, 1999). For the Colorado River basin, these investigators found that mean anomalies in snowmelt discharge and annual runoff during El Niño years depict a transition between drier-than-average conditions in the north, and wetter-than-average conditions in the Southwest. Associations during La Niña years are generally opposite those in El Niño years. Cayan and Webb (Cayan and Webb, 1992) reported that the largest river flows (floods) in the Southwestern United States this century have occurred during El Niño years, which are frequently characterized by severe winter frontal storms or by intense summer thunderstorms (and even some tropical storms that find their way up from the west coast of Mexico). In other areas of the Southwestern United States where snowmelt is the primary source for streamflow, a few intense storms typical of El Niño years may not cause high river flows.

2.2. South America

Molinier et al. (Molinier et al., 1999) compared discharge records at 50 stations across the Amazon basin with equatorial Pacific sea surface temperature (SST) and found a strong correlation between high discharge years and ENSO events for much of the basin, with the exception of the southwestern and northeastern regions of the Amazon. Marengo (Marengo, 1999) analyzed precipitation and discharge data for the Amazon basin since the mid-1920s and found the same decline in discharge rates over the past two decades (1980s and 1990s), as also reported by Ordoñez Galvez (Ordoñez Galvez, 1999). These authors reported 10- and 30-yr cycles that correlate well with the equatorial Pacific SST. Dettinger et al. (Dettinger et al., 2000) reported that ENSO indices of climate account for about 15% of river discharge rates in the Americas, with the strongest correlations in the rivers of tropical South America east of the Andes. Piovano et al. (Piovano et al., 1999) reported a strong correlation between the ENSO-related Pacific SST anomalies and large deviations from mean monthly discharges for the upper Parana River in Brazil. Amarasekera et al. (Amarasekera et al., 1997) found the correlation between ENSO and annual discharge rates on the Parana River to be twice as strong as the correlation between ENSO and annual discharge rates on the Amazon River. Robertson et al. (Robertson et al., 2001) reported that 17-yr, 8-yr, and ENSO oscillatory components were associated with statistically significant changes in the probability distribution of monthly flows on the Parana River at Corrientes.

In Chile and central-western Argentina, north of 40°S, streamflows were normal or above normal during El Niño years and well below normal during La Niña years (Compagnucci and Vargas, 1998). Heredia Calderon and Pombosa (Heredia Calderon and Pombosa, 1999) investigated ENSO signals in the discharge records of three dammed Ecuadorian rivers: the Napo, Paute, and Esmeraldas. They found a strong interannual ENSO signal on the Esmeraldas River, on the western slope of the Andes, but a weak effect on the Napo and Paute Rivers, which are part of the Amazon drainage basin. However, ENSO was associated with a seasonal shift in precipitation patterns in the two Amazon tributaries, with an earlier peak and reduced duration of the annual flood. A similar pattern was found by Ronchail (Ronchail, 1999) on the Rio Madiera in Bolivia, where precipitation in the Andean portion of the basin was highly sensitive to ENSO while rainfall in the lowlands to the east was not. As a result, the ENSO signal in the runoff record may be rapidly attenuated in the downstream direction.

2.3. Eurasia, Africa, and Australia

Variations in river flow from year to year are more strongly related to precipitation changes than to temperature changes in Eurasia (Krasovskaia, 1995). In northern Siberia, recent increases in temperature have had little effect on flow timing because precipitation continues to fall as snow (Shiklomanov, 1994). Decreases in spring river discharge and increases in winter, summer, and autumn runoff have been reported since the mid-1970s for Eurasian basins (Georgiyevsky et al., 1996).

Over the past four decades, the NAO pattern has gradually altered from the most extreme and persistent negative phase in the 1960s to an extreme positive phase during the late 1980s and early 1990s—a trend that has been responsible for relatively mild and wet winters during the latter period over much of northwest Europe (Hurrell and van Loon, 1997) in association with major flood events (Kundzewicz and Takeuchi, 1999). For the Lena River in Siberia, Yang et al. (Yang et al., 2002) reported significant changes in various components of the hydrologic regime over the past several decades related to air temperature and summertime rainfall.

A strong linkage between ENSO, rainfall, and streamflow has been documented for many parts of eastern Australia (Whetton et al., 1988; Simpson et al., 1993; Chiew et al., 1998).

For Africa, Molinier et al. (Molinier et al., 1999) reported that discharge records for the Congo basin were correlated well with SST anomalies in the southern Atlantic, rather than the equatorial Pacific Ocean. Eltahir (Eltahir, 1996) reported that ENSO events affect flows of the Nile River, indicating drought in highland Ethiopia, which is a source of 85% of the Nile's water. Sircoulon (Sircoulon, 1990) reported decreases in river flow since the 1970s in several African rivers.

3. Hydrologic data sources

3.1. River discharge records

Monthly river discharge (DIS) records for 30 of the world's largest river basins were obtained from the River Discharge Database (RivDIS; Vörösmarty et al.,

Table 1. Thirty major river systems selected for study of historical discharge records.

River system	Continent	Length (km)	Discharge into sea or ocean	STN-30 basin area (km^2)
Nile	Africa	6727	Mediterranean Sea	3 826 122
Amazon	South America	6308	Atlantic Ocean	5 853 804
Mississippi	North America	6228	Gulf of Mexico	3 202 959
Ob′	Asia	5566	Kara Sea	2 570 131
Yenisei-Angara	Asia	5536	Kara Sea	2 582 221
Congo (Zaire)	Africa	4667	Atlantic Ocean	3 698 803
Amur	Asia	4506	Pacific Ocean	2 902 865
Paraná	South America	4498	Atlantic Ocean	2 661 392
Lena	Asia	4345	Laptev Sea	2 417 937
Mackenzie	North America	4248	Beaufort Sea	1 712 738
Niger	Africa	4184	Atlantic Ocean	2 240 019
Saint Lawrence	North America	3782	Atlantic Ocean	1 266 642
Volga	Europe	3701	Caspian Sea	1 463 315
Yukon	North America	3540	Pacific Ocean	852 029
Euphrates–Tigris	Asia	2889	Persian Gulf	967 341
Danube	Europe	2816	Black Sea	788 002
Ganges (Brahmaputra)	Asia	2736	Indian Ocean	1 628 405
Amu-Darya	Asia	2494	Aral Sea	508 839
Ural	Asia	2494	Caspian Sea	296 283
Kolyma	Asia	2414	East Siberian Sea	665 674
Colorado (Arizona)	North America	2333	Pacific Ocean	807 573
Dnieper	Europe	2285	Black Sea	508 839
Orange	Africa	2092	Atlantic Ocean	943 577
Columbia	North America	1947	Pacific Ocean	724 025
Don	Europe	1931	Black Sea	423 038
Petchora	Europe	1802	Barents Sea	301 599
Indigirka	Asia	1770	East Siberian Sea	323 710
Senegal	Africa	1609	Atlantic Ocean	847 273
Volta	Africa	1609	Atlantic Ocean	398 071
Godavari (Godavary)	Asia	1448	Indian Ocean	311 575

1998). A major river basin was characterized for this study as one with a total drainage area of at least 300 000 km^2 and whose mouth opens into an ocean or sea (Table 1). One pair of RivDIS station records was selected to represent each major river basin. The station site A of each pair was selected for its location as close as possible to the source of the river, whereas station site B of each pair was selected for its location as close as possible to the mouth of the river (Table 2). The station discharge records largely cover the period from 1950 to 1988. Only stations with at least 9 continuous years of monthly station discharge records were considered as candidates for selection in our study. Of the 60 selected stations, 50 offered at least 19 yr of continuous station discharge records. The mean number of years of complete monthly discharge records for the 60 selected stations was 23.2 yr with a standard deviation of 6.4 yr. Basins for which one of the two selected stations offered less than 19 yr of continuous station discharge records were the Nile, Kolyma, Ural, Don, Colorado (Arizona), and Columbia Rivers. Only the

Table 2. Locations of paired RivDIS station sites A and B within major river basins.

River system	Site A				Site B			
	RivDIS station	Lat +N/−S	Lon +E/−W	Percentage area of entire STN-30 basin	RivDIS station	Lat +N/−S	Lon +E/−W	Percentage area of entire STN-30 basin
Nile	1487	23.96	32.90	93.1	1159	29.71	31.26	97.4
Amazon	11466	−3.08	−67.93	20.8	514	−1.91	−55.55	81.4
Mississippi	387	38.88	−90.16	56.6	385	32.31	−90.90	92.2
Ob′	878	56.58	84.87	2.2	835	66.57	66.53	98.2
Yenisei-Angara	886	62.22	92.02	8.2	880	67.48	86.50	92.7
Congo (Zaire)	10	4.37	18.50	12.8	1534	−4.30	15.30	99.7
Amur	169	45.01	133.65	3.2	932	50.63	137.12	95.8
Paraná	516	−24.06	−54.26	31.0	960	−27.46	−58.85	81.5
Lena	165	59.55	126.95	0.9	930	70.89	127.41	98.4
Mackenzie	280	59.86	−111.58	35.5	267	65.28	−126.86	89.0
Niger	61	12.86	−7.55	5.0	1513	11.88	3.40	64.1
Saint Lawrence	300	46.51	−84.36	0.7	311	45.00	−74.78	46.2
Volga	817	48.76	44.72	91.0	1460	48.30	46.00	92.4
Yukon	263	62.10	−136.26	10.0	1203	64.74	−155.48	77.6
Euphrates–Tigris	801	38.82	38.77	5.7	811	33.83	42.72	32.0
Danube	752	48.67	13.12	5.5	765	45.18	28.80	98.6
Ganges (Brahmaputra)	883	26.13	91.70	25.5	863	24.83	87.92	58.1
Amu-Darya	136	37.53	71.51	3.4	1252	42.28	59.7	100
Ural	130	50.28	57.15	0.7	826	50.85	51.28	65.1
Kolyma	176	64.18	151.30	1.0	937	67.37	153.67	53.4
Colorado (Arizona)	360	36.86	−111.58	34.8	1072	32.66	−114.65	98.2
Dnieper	808	51.45	31.37	19.6	805	47.92	35.15	92.6
Orange	1518	−26.82	28.06	4.7	1459	−28.71	17.51	88.7
Columbia	356	46.43	−117.16	0.3	353	45.60	−121.18	90.7
Don	130	50.28	57.15	0.5	815	47.50	40.67	76.9
Petchora	830	66.65	59.1	15.4	829	65.47	52.25	76.7
Indigirka	175	61.68	144.66	4.9	936	69.58	147.35	91.8
Senegal	1510	13.14	−10.48	8.9	70	14.90	−12.45	69.6
Volta	1543	10.57	−2.92	20.5	1494	8.15	−2.03	30.5
Godavari (Godavary)	1261	18.83	79.45	32.9	858	16.92	81.78	97.4

Euphrates–Tigris basin offered two stations with between 9 and 19 yr of continuous station discharge records.

We note that several major river basins were eliminated from consideration by the selection criteria of having two different RivDIS station records well-spaced toward the source and the mouth of the river drainage plus 9 continuous years of monthly station discharge for both stations. Those major basins (all with total drainage area of at least 1 000 000 km^2; Vörösmarty et al., 2000) that did not meet our criteria for selection included the Zambezi, Chang Jiang, Chari, Indus, Nelson, Orinoco, and Murray Rivers.

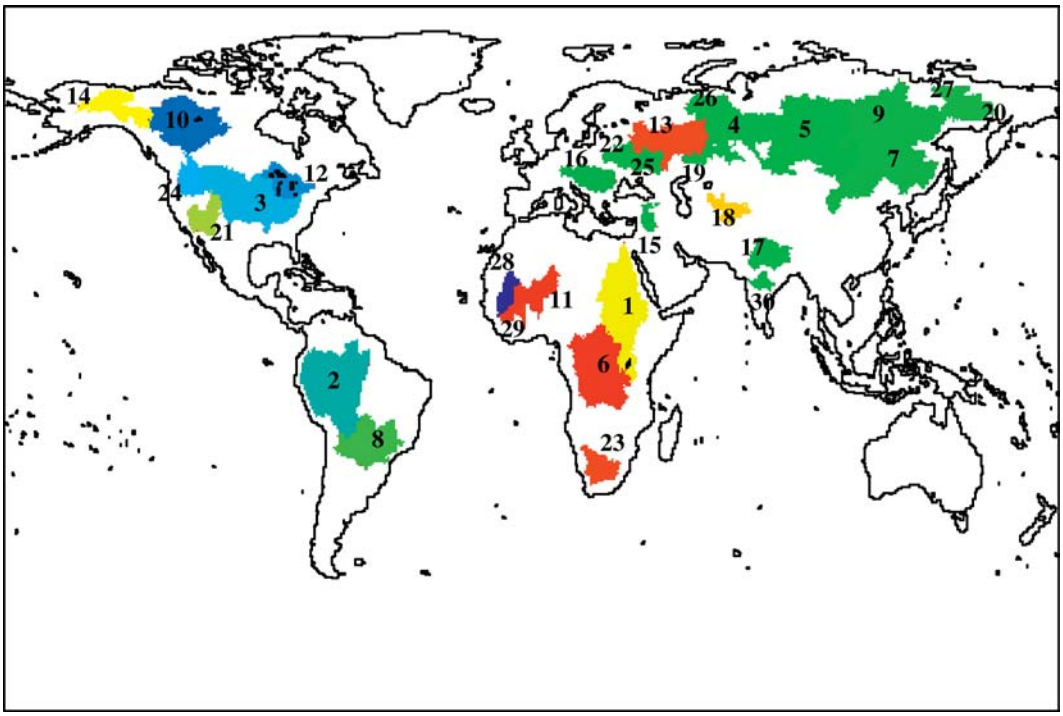

Figure 1. River basin areas for site B discharge station locations (relatively close to the river mouth), delineated from the STN-30 flow direction dataset (Vörösmarty et al., 2000). Key to river basin names: 1 Nile, 2 Amazon, 3 Mississippi, 4 Ob′, 5 Yenisei-Angara, 6 Congo (Zaire), 7 Amur, 8 Paraná, 9 Lena, 10 Mackenzie, 11 Niger, 12 Saint Lawrence, 13 Volga, 14 Yukon, 15 Euphrates–Tigris, 16 Danube , 17 Ganges, 18 Amu-Darya, 19 Ural, 20 Kolyma, 21 Colorado (Arizona), 22 Dnieper, 23 Orange, 24 Columbia, 25 Don, 26 Petchora, 27 Indigirka, 28 Senegal, 29 Volta, 30 Godavari (Godavary).

3.2. River basin delineation

Basin areas were delineated in the Simulated Topological Network 30-min resolution (STN-30) dataset from Vörösmarty et al. (Vörösmarty et al., 2000). Using the STN-30 flow direction dataset, we further delineated the subbasin (upstream) drainage area from the locations of both RivDIS sites A and B (Figure 1) within each major river basin.

The site A subbasins (near the river source) were intentionally selected to cover relatively small upland drainage areas, compared to either the site B subbasins (nearer the river mouth) or to the entire STN-30 basin area. The exceptions to this pattern are the Nile, Mississippi, and Volga Rivers (for which we could not locate extended RivDIS datasets that were farther upstream than these). Furthermore, all of these site A subbasins show less than 3% area as being irrigated (Döll and Siebert, 2000), with the exception of the Mississippi, Don, and Godavari River basins. This means that the site A discharge records should represent relatively "natural" signals of climate or some other geophysical controls over surface water

flows for the globe, as opposed to including extensive human effects on the discharge history.

The site B subbasins (nearer the river mouth) were intentionally selected to cover relatively large portions (nearly 50% or more) of the entire STN-30 basin area. The only exceptions to this pattern are the Euphrates–Tigris and the Volta River site B subbasins at about 30% total STN-30 basin coverage (for which, again, we could not locate extended RivDIS datasets that were farther downstream than these). Several of these site B subbasins show more than 3% area as being irrigated (Döll and Siebert, 2000), notably the Mississippi, Euphrates–Tigris, Danube, Ganges, Amu-Darya, Columbia, and Godavari River basins.

3.3. Land surface climate

For comparisons to RivDIS records, historical land climate datasets for 30-min resolution monthly PREC and air surface temperature were obtained from interpolated weather station records covering the period 1958–98 (New et al., 2000). The aggregate PREC amount falling over all 0.5 cells within a given drainage basin represents the gross monthly atmospheric input of water to that basin. A portion of this gross PREC input flux is lost back to the atmosphere within the same month as PET flux, resulting in a net atmospheric input water flux to the basin area, computed as PREC − PET with a minimum monthly value of zero. We computed monthly PET flux from air surface temperature (New et al., 2000) according to the method of Thornthwaite (Thornthwaite, 1948), as documented in Potter and Klooster (Potter and Klooster, 1999). These estimated PET methods have been validated in numerous different climate zones (Potter et al., 2001; Federer et al., 1996). The complete algorithm we have used is actually equivalent to PREC − ET because the minimum allowed value of the difference is zero (i.e., there can be no ET greater than the available PREC).

3.4. Climate indices

The influence of ocean surface climate events, such as ENSO, on atmospheric circulation and land surface climate have been noted as a significant global teleconnection (Glantz et al., 1991). Teleconnection is a term used in meteorological studies to describe simultaneous variation in climate and related processes over widely separated points on earth. There are different phases in CIs such as the ENSO, which is called El Niño in the warm phase and La Niña in the cold phase. ENSO warming at the sea surface, which is driven by changes in winds and ocean–atmosphere heat exchange, typically extends to about 30°N–30°S latitude with lags into continental land areas of several months. The Southern Oscillation index (SOI) is an indicator of atmospheric impacts of ENSO, computed as the standardized difference between sea level pressure (SLP) measured in Tahiti (17°S, 149°W) and Darwin, Australia (13°S, 131°E). Other indices for ENSO include the Niño1+2 delineated by the SST between 0°–0° and 90°–80°W in the eastern tropical Pacific, and Niño3+4 delineated by the SST between 5°N–5°S and 170°–120°W in the western tropical Pacific.

The SOI, Niño1+2, and Niño3+4 indices are commonly used to document warm phases in ENSO, which are often associated with above-average temperatures in

the northwestern half of the North American continent, and below-average temperatures in the southeastern half (Trenberth and Hurrell, 1994; Klein et al., 1999; McCabe and Dettinger, 1999). There is also a pattern of the warm-phase ENSO associated with above-average precipitation over western coastal South America (Vuille et al., 2000), the southern United States, and northern Mexico, plus below-average precipitation in south-central Africa, northeastern South America, parts of southern Asia and Australia, and in North America from the Canadian Rockies to the Great Lakes region.

The NAO index refers to the north–south oscillation in atmospheric mass between the Icelandic low (65°N, 22°W) and the Azores high pressure centers from 39°N, 9°W to 36°N, 6°W (Walker and Bliss, 1932). The atmospheric state indexed by negative NAO corresponds to a southward displacement of winter storms and moisture transport across the North Atlantic into southern Europe (Hurrell, 1995). A positive NAO corresponds to a northward displacement of storms and moisture in northernmost Europe and Russia. During winters when the NAO index is high, anomalously low precipitation commonly occurs over the Canadian Arctic, central and southern Europe, the Mediterranean, and the Middle East. In contrast, anomalously high precipitation occurs from Iceland through Scandinavia. In the eastern United States, winters with negative NAO are characterized by more northerly winds, which reduce moisture transports into the region from the south. The NAO can also represent the persistence of below-average temperature variations over North Africa and the Middle East, and above-average temperatures over North America (Hurrell, 1995).

4. Methodology

A scheme was developed to characterize major rivers on the basis of results from our correlation analysis by defining categories for associations of DIS records with net PREC inputs, CIs, and human water use patterns. Following an assessment of intrabasin (paired site A versus site B correlation) patterns, we first characterize major rivers on the basis of the strength of localized climate control (PREC − PET) over historical DIS rates (Figure 2). The next grouping of rivers is on the basis of the strength of teleconnections to CIs. Finally, rivers groupings are characterized on the basis of their association with land and water use patterns within the site A and site B drainage areas.

Prior to correlation analysis, a *Z*-score normalization was applied to all variable time series datasets, whereby all monthly values were transformed into a standard deviation value based on the long-term monthly mean of that variable time series. We note that although many of the absolute area totals for the site A subbasins are not large, this does not affect our interpretation of the results from correlations with climate time series because the *Z*-score normalization approach removes the effect of actual flow volumes (small or large) from the basin-to-basin comparisons of correlation *r* values, and accounts only for relative deviations from the long-term monthly mean flow rates. The *Z*-score normalization also removes any strong seasonal patterns in the climate and discharge rates, such as those documented by Dettinger and Diaz (Dettinger and Diaz, 2000) for hundreds of major rivers,

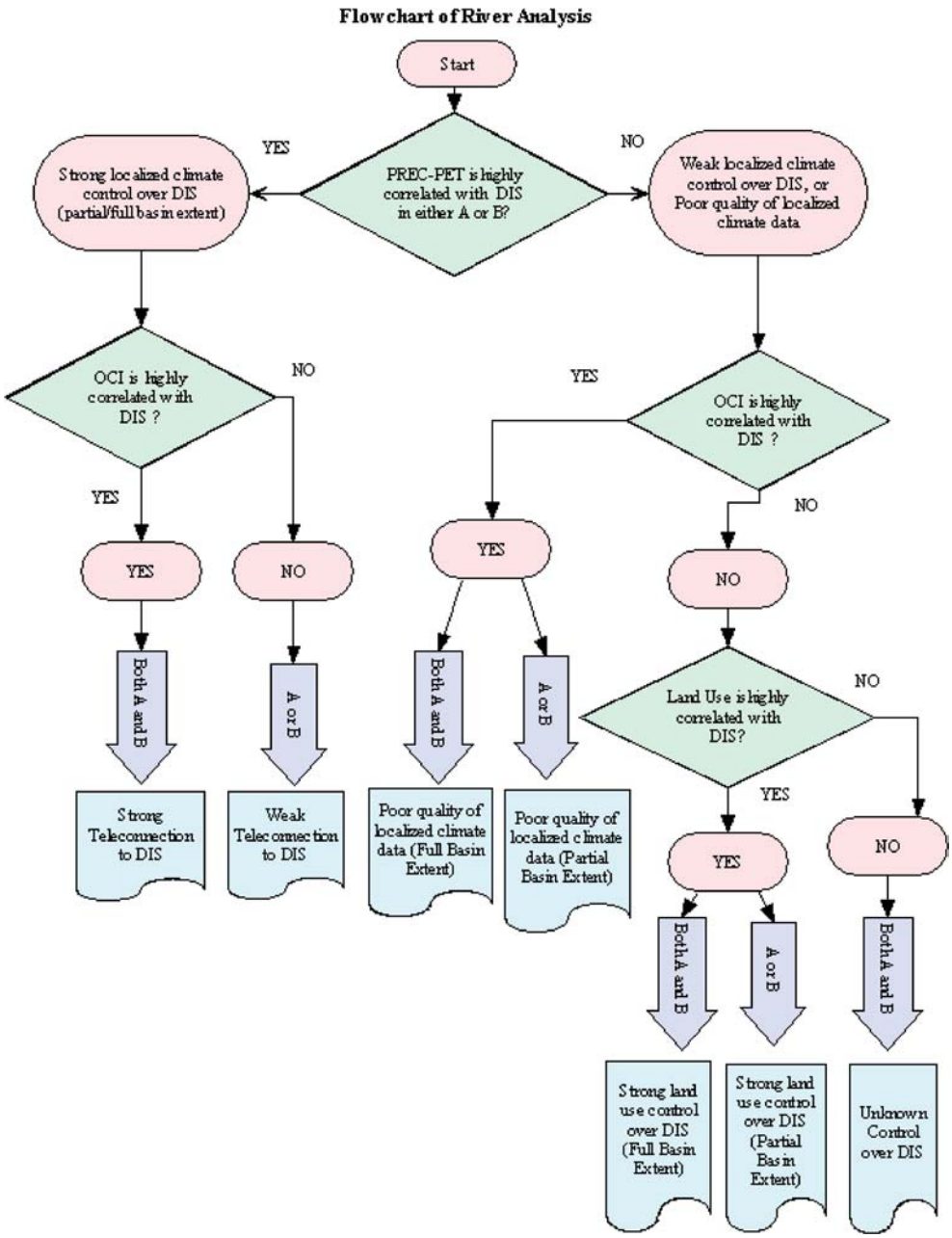

Figure 2. Flowchart to characterize major rivers on the basis of correlations of historical DIS records with net PREC inputs, CIs, and human land/water use patterns. YES means a significant correlation is found between climate or land/water use and a site A and/or site B DIS record, while NO means a significant correlation is not found.

leaving relative deviations within the DIS time series to correlate with relative deviations in local or global climate patterns.

In river basins where difference between (PREC – PET) and historical DIS rates is seasonal, and the yearly sum may be close to zero, several factors could be at work that are only indirectly related to localized climate control: (i) the time lag required for the deep drainage water to reach the stream; (ii) the time lag necessary for the water to flow downstream in the river; and (iii) delay between snowfall and snowmelt (midlatitude basins only). To account for these factors, seasonal phase shifts in climate data of up to 12 months were applied wherever there was a need to improve correlations with (lagged) historical DIS records.

The Pearson product-moment correlation coefficient (r) was used as a test of significant association between two time series. Statistical significance of correlations is dependent on the number of observations considered independent in a time series dataset. In all cases, the significance levels of a correlation were determined on the basis of degrees of freedom equal to $n - 2$ years for each discharge station record. For example, with a sample size of $n = 19$ yr, which conservatively minimizes all temporal autocorrelation effects in monthly discharge and climate time series data, any value of the Pearson product-moment correlation coefficient of $r > 0.38$ or $r > 0.46$ can be considered significant at the $p < 0.1$ and $p < 0.05$ confidence levels, respectively (i.e., two-tailed test of significance).

5. Results and discussion

5.1. Intrabasin discharge patterns

Intrabasin correlation analysis was conducted to determine where any relatively natural discharge signals represented in site A records are (or are not) sustained, and perhaps amplified or dampened, in the larger site B basin discharge signals. Up to a 12-month shift was used for these correlations. The majority (19 of 30) of intrabasin site A versus site B correlations were significant ($p < 0.1$), with the exception of the paired discharge records for the Amazon, Amur, Brahmaputra, Colorado (Arizona), Ob′, Orange, Saint Lawrence, Ural, Volga, Yenisei-Angara, and Yukon Rivers. The implication is that there has been alterations in the runoff generation processes for these 11 rivers to sufficiently decouple the discharge signals represented in site A records from the larger site B basin discharge signals. In contrast, the highest intrabasin discharge correlations (at $r > 0.7$) were found for the Columbia, Godavari, Parana, Petchora, and Senegal Rivers, indicating that either 1) the relatively natural discharge signals represented in site A have been little altered throughout the larger basin area for these rivers, or 2) human management of discharge signals representing the drainage area for site A have been maintained throughout the larger basin area represented by site B discharge signals.

5.2. Correlations between climate and discharge rates

Following the analysis scheme presented in Figure 2, major river basins can be grouped according to the strength of localized climate control (PREC – PET) over historical DIS rates. We find that for six major river basins, historical DIS

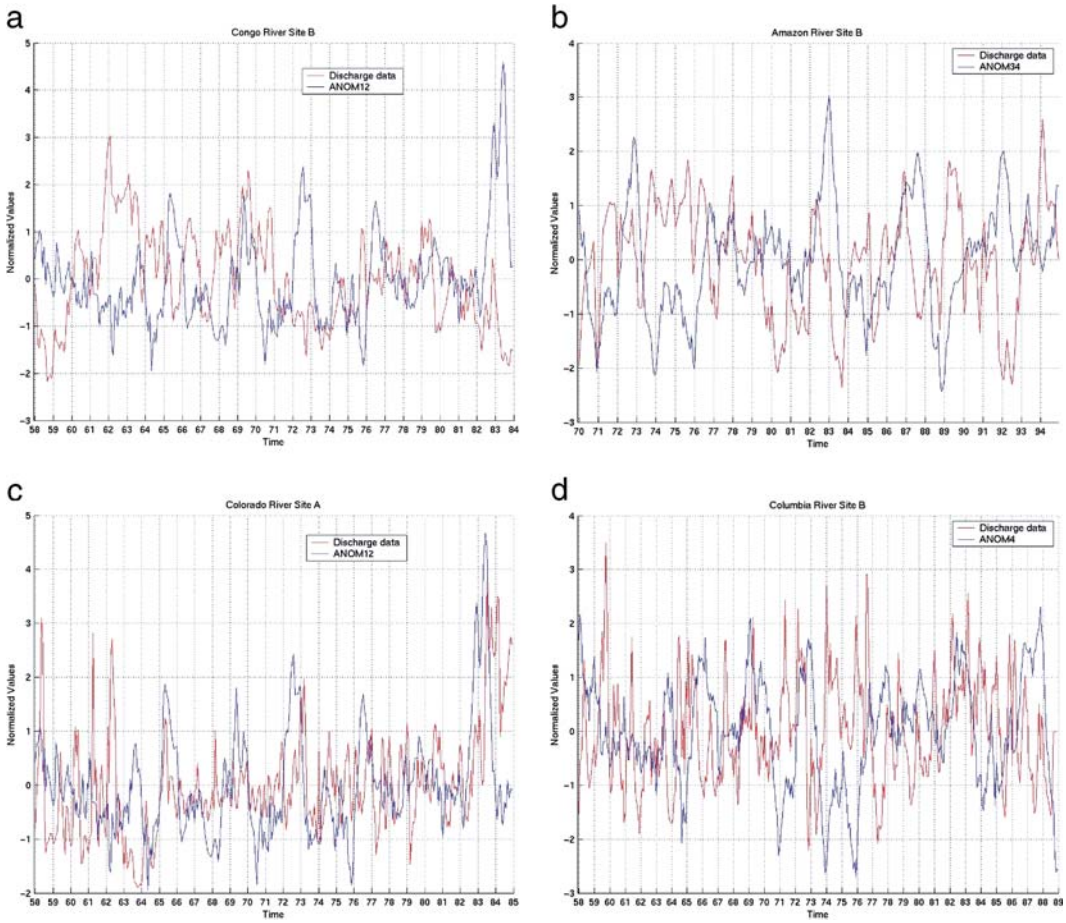

Figure 3. Time series plots of river discharge and climate index anomalies. (a) $r = -0.34$, $p < 0.1$. (b) $r = -0.5$, $p < 0.05$. (c) $r = +0.38$, $p < 0.1$. (d) $r = -0.34$, $p < 0.1$.

anomalies are significantly correlated ($p < 0.05$ in most cases) with (PREC − PET) anomalies for both site A and site B discharge station records indicating strong localized climate control over the full drainage basin extent. These rivers are the Congo (Zaire), Danube, Dnieper, Mississippi, Niger, and the Volta. Of these six, only the Congo (Zaire) River showed a significant ($r = -0.34$, $p < 0.1$) correlation (Figure 3a), and hence a moderately strong teleconnection with the Niño1+2 anomaly record to historical DIS anomalies. No significant correlations could be detected between the NAO and any historical DIS station records used in this study.

We find that for the additional seven river basins, historical DIS anomalies are significantly correlated ($p < 0.1$) with (PREC − PET) anomalies for either site A or site B discharge station records, but not for both, suggesting moderately strong localized climate control over the partial basin extent. These rivers are the Amazon (site B), Amur (site A), Euphrates–Tigris (site A), Godavari (site B), Parana (site

A), Senegal (site B), and the Volga (site A). Of these seven, only the Amazon River (site B) showed significant ($r = -0.5$, $p < 0.05$) correlation (Figure 3b), and hence a strong global teleconnection with the Niño3+4 anomaly record to historical DIS anomalies.

The remaining 17 major river basins all showed weak localized climate controls (PREC − PET) over both site A and site B discharge station records. Of these 17, only two rivers, the Colorado (Arizona) (site A) and the Columbia (site B), showed significant ($p < 0.1$) correlations, and hence moderately strong teleconnections with the Niño1+2 and Niño4 anomaly records (Figures 3c and 3d), respectively, to historical DIS anomalies. Based on these results, we hypothesize that the historical gridded PREC and PET climate data for the Colorado (Arizona) (site A) and the Columbia (site B) subbasins are not of the quality required to detect localized climate controls over DIS rates.

5.3. Potential impacts of land use on discharge rates

We hypothesize that the weak teleconnection of any CI with historical DIS rates in the remaining 17 major river basins means that there may have been important land/water use controls by human populations in these drainage basins, which have been sufficient to partially uncouple PREC − PET water inputs from station discharge rates. We can document, for example, that the site B subbasins for the Amu-Darya, Ganges, and Columbia Rivers had between 3% and 20% of the area irrigated by the early 1990s (Döll and Siebert, 2000). This leaves 13 river basins out of a total of 30 lacking an explanation for the uncoupled PREC − PET water inputs with station discharge rates.

Historical changes in cropland coverage have been mapped by Ramankutty and Foley (Ramankutty and Foley, 1999) at 0.5° spatial resolution for the global land surface. According to this data source, the river basins that have experienced area increases of +2% (or much greater) in cropland coverage in the site B subbasin over the period 1950–92 were the Amu-Darya, Ganges, Dnieper (+20%), Euphrates–Tigris, Nile, Ob′, Parana, Ural (+19%), Volga (+11%), and the Volta. Two other rivers experienced a decline in cropland area coverage in the site B subbasin over the period 1950–92, namely, the Godavari (–2%) and the St. Lawrence (–6%). If changes in cropland coverage within a drainage basin are related, even indirectly, to changes in historical DIS rates, then this leaves 9 out of a total of 30 river basins that lack explanations for the uncoupled PREC − PET water inputs with station discharge rates.

It is plausible that historical gridded PREC and PET climate data for these nine remaining river basins are not of the high quality required to detect localized climate controls over DIS rates. For example, most of these nine river basins are in relatively remote areas of the high-latitude or high-elevation zones, such as the Indigirka, Kolyma, Lena, Mackenzie, Orange, Petchora, Yenisei-Angara, and Yukon Rivers, where there may be (too) few weather stations for generation of reliable interannual grids for PREC and PET variables. This potential problem with the quality of PREC inputs for explaining historical DIS record was also reported by Dettinger and Diaz (Dettinger and Diaz, 2000), as was the possible effect of the complex dynamics of snowmelt contribution within these high-latitude basins.

Snowpack formation and snowmelt could act to decouple simple PREC anomalies and historical DIS relationships, although our inclusion of up to 12-month lag times in the climate–DIS anomaly correlations should account for regularly delayed effects of snowmelt on peak runoff timing. A 2- or 3-month variability of spring peaks in runoff due to snowmelt timing, as reported for these high-latitude basins by Dettinger and Diaz (Dettinger and Diaz, 2000), would not be well accounted for even using the lag time settings for our correlations. This point is reinforced by the results of Yang et al. (Yang et al., 2002) for the Lena River, whose historical discharge rates were not significantly correlated with precipitation rates in cold months. Gradual long-term warming trends may have more significant control on river ice thickness and melt rates in these high-latitude basins.

Nevertheless, to test the possibility that a variability of 2 or 3 months in spring peaks for river runoff are attributable to the timing of snowmelt, we checked the time series correlations between PET and DIS anomalies for the several river basins listed above that are located in relatively remote areas of the high-latitude zones. Because the PET algorithm we use is an empirical transformation of monthly air surface temperature, year-to-year variability in climate conditions that influence the timing of snowmelt should be related to these PET estimates. However, results show that none of the r values for correlations between PET anomalies and site B DIS anomalies are significant (at $p < 0.1$) for the high-latitude river basins listed above. Only the Amazon, Godavari, and Orange Rivers showed significant ($r = -0.4$ $p < 0.1$) correlations between PET anomalies and site B DIS anomalies. Consequently, controls on historical DIS anomalies remain uncertain for the high-latitude river systems.

5.4. Other potential controls on discharge rates

It is commonly observed that large river systems not only have delayed discharge signals (relative to the timing of precipitation) but can also attenuate the discharge signal, for example, due to storage and differential release in soils, lakes, reservoirs, and wetlands. Attenuation controls like these may reduce the correlation between discharge rates at distant site locations within a major basin and/or large-scale climate patterns. Consequently, there may be several natural processes at work, in addition to anthropogenic effects, to explain the lack of correlation we reported above in several basin cases.

An interesting case is the St. Lawrence River basin, where the Great Lakes have the potential to attenuate discharge signals, due to the water residence time of several decades in the lakes. Ice damming and flooding may similarly affect the Amur, Ob′, Yenisei, and Yukon basin discharge records, creating areas that can flood to create large lakes. Climate variations in the high northern latitudes over the past several decades have been linked to earlier spring thaws, major breaks in ice dams, and melting of glaciers (Dyurgerov and Meier, 1997; Magnuson et al., 2000; Serreze et al., 2000), which are not accounted for in our analysis so far.

Finally, the influence of man-made dams, particularly on the Colorado, Columbia, Danube, Orange, Parana, and Volga Rivers, cannot be discounted. For each of these basins, we searched the RivDIS archive to determine if there

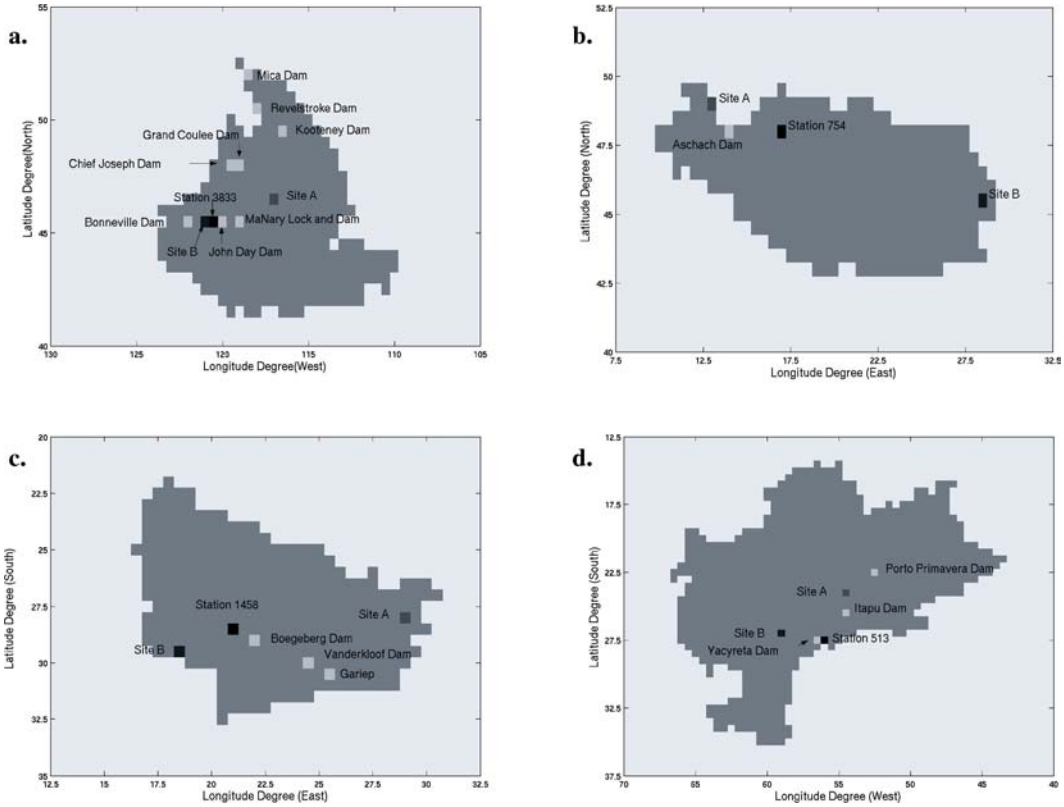

Figure 4. Spatial relationships between selected DIS sites and major dam locations in the (a) Columbia, (b) Danube, (c) Orange, and (d) Parana River basins.

were large dams located between our chosen site A and site B locations, and if there is also a third DIS station record located between the dam location(s) and the site B location. If this is true, then it is feasible to determine if the site B DIS record is more similar (higher correlation value, shorter shift period) to the third DIS station record, compared to the site A DIS record. If the answer is yes, then it is plausible that the dam has had a notable impact on the site B DIS pattern and potentially on all discharge moving toward the mouth of the river basin. If the answer is no, then the dam has had no detectable impact on the site B DIS pattern, relative to the discharge record at locations upstream from the dam location. Nonetheless, it is conceivable that dams or land use located upstream of the site A location have major impacts on all discharge moving toward the mouth of the river basin.

The following four rivers were determined to have all the requisite discharge records for evaluation of dam effects as described above: Columbia, Danube, Orange, and Parana. The spatial relationships between selected DIS sites and major dam locations are shown in Figure 4. Correlation analysis implied that dams have had a notable impact on the site B DIS pattern in the Orange and Parana River

Table 3. Correlation values (*r*) for site A–site B and third DIS–site B (best shift, months) in river basins with potential impacts of dams on historical discharge.

River (third DIS ID)	*r* site A–site B	*r* third DIS–site B	(Dam name) impact
Columbia (3833)	0.75 [0]	0.52 [0]	(Mica) low
Danube (204)	0.54 [0]	0.56 [0]	(Aschach) low
Orange (1458)	0.23 [4]	0.85 [0]	(Gariep) high
Parana (513)	0.76 [0]	0.92 [0]	(Itaipu) medium

basins (Table 3). For instance, site A in the Parana basin is located after a series of dams that highly regulate the Parana flow, while site B is just downstream of the confluence of the Parana and the Paraguay Rivers. The Paraguay River crosses a large flat region that floods seasonally. Hence, sites A and B can have a similar hydrological signature (damped yearly hydrograph), but for potentially different reasons.

For the Columbia and Danube basins, the selected dam had little detectable impact on the site B DIS pattern, relative to the discharge record at locations upstream from the dam location. However, we cannot rule out the influence of dams and river water use located farther upstream from site A DIS stations, which could have altered discharge patterns throughout both of these basins.

6. Conclusions

- Discharge signals represented in upstream RivDIS station records are sustained in the downstream RivDIS station records for nearly two-thirds of the 30 major river drainages selected.
- Net monthly precipitation anomalies (PREC − PET) can explain the historical interannual patterns in monthly river discharge for nearly one-half of the 30 major river drainages selected from the RivDIS dataset.
- River basins that show the strongest, most easily predicted local climate control over historical DIS rates are located mainly in the seasonally warm temperate and tropical latitude zones, as opposed to river basins located mainly in the higher-latitude zones (above 45°N), for which localized (PREC − PET) controls cannot be readily detected using the gridded datasets available.
- Climate indices such as the Niño1+2 and Niño3+4 anomalies correlate highly with historical interannual anomalies in monthly river discharge for only four of the selected RivDIS station records, namely, on the Amazon, Congo (Zaire), Columbia, and Colorado (Arizona) Rivers. Our teleconnection results are not as strong nor as extensive as those reported by Dettinger and Diaz (Dettinger and Diaz, 2000), who depicted high levels of statistical significance for RivDIS station correlations with ENSO indices worldwide.
- Historical patterns of cropland development and irrigated areas along major river systems may have strongly affected interannual patterns in monthly river discharge rates for at least one-third of the 30 major river drainages selected from the RivDIS dataset.

Acknowledgments. This work was supported by grants from NASA programs in Intelligent Systems and Intelligent Data Understanding, and the NASA Earth Observing System (EOS) Interdisciplinary Science Program. The authors thank Michael Coe and Dennis Lettenmaier for comments on an earlier version of the manuscript.

References

Amarasekera, K.N., R.F. Lee, E.R. Williams, and E.A.B. Eltahir, 1997: ENSO and the natural variability of tropical rivers. *J. Hydrol.,* **200,** 24–39.

Barros, A.P., and J.L. Evans, 1997: Designing for climate variability. *J. Profess. Issues Engineer. Educ. Practice,* **123,** 62–65.

Caddy, J. F., and A. Bakun, 1994: A tentative classification of coastal marine ecosystems based on dominant processes of nutrient supply. *Ocean Coast Manage.,* **23,** 201–211.

Cayan, D. R., and R. H. Webb, 1992: El Niño/Southern Oscillation and streamflow in the western United States, in *El Niño: Historical and Paleoclimatic Aspects of the Southern Oscillation*, edited by H. F. Diaz and V. Markgraf, Cambridge University Press, 29–68.

Cayan, D.R., K. T. Redmond, and L. G. Riddle, 1999: ENSO and hydrologic extremes in the western United States. *J. Clim.,* **12,** 2881–2893.

Chiew, F.H.S., T.C. Piechota, J.A. Dracup, and T.A. McMaho, 1998: El Niño-Southern Oscillation and Australian rainfall, stream flow, and drought—Links and potential for forecasting. *J. Hydrol.,* **204,** 138–149.

Clark, M.P., M. C. Serreze, and G. J. McCabe, 2001: Historical effects of El Niño and La Niña events on the seasonal evolution of the montane snowpack in the Columbia and Colorado River Basins. *Water Resour. Res.,* **37,** 741–758.

Coe, M.T., 2000: Modeling terrestrial hydrologic systems at the continental scale: Testing the accuracy of an atmospheric GCM. *J. Clim.,* **13,** 686–704.

Compagnucci, R. H., and W. M. Vargas, 1998: Interannual variability of the Cuyo River's streamflow in the Argentinian Andean mountains and ENSO events. *Int. J. Climatol.,* **18,** 1593–1609.

Dettinger, M., and H. Diaz, 2000: Global characteristics of stream flow seasonality and variability. *J. Hydrometeorol.,* **1,** 289–310.

Dettinger, M., D. Cayan, G. J. McCabe, and J. Marengo, 2000: Multiscale streamflow variability associated with El Niño/Southern Oscillation, in *El Niño and the Southern Oscillation—Multiscale Variability and Global and Regional Impacts*, edited by H. F. Diaz and V. Markgraf, Cambridge University Press, 113–146.

Döll, P., and S. Siebert, 2000: A digital global map of irrigated areas. *ICID J.,* **49** (2), 55–66.

Driscoll, N.W., and G. H. Haug, 1998: A short circuit in thermohaline circulation: A cause for Northern Hemisphere glaciation? *Science,* **282,** 436–438.

Dyurgerov, M.B., and M.F. Meier, 1997: Mass balance of mountain and subpolar glaciers: A new global assessment for 1961–1990. *Arct. Alp. Res.,* **29,** 379–391.

Eltahir, E.A., 1996: El Niño and the natural variability in the flow of the Nile River. *Water Resour. Res.,* **32,** 131–137.

Federer, C. A., C. J. Vörösmarty, and B. Fekete, 1996: Intercomparison of methods for potential evapotranspiration in regional or global water balance models. *Water Resour. Res.,* **32,** 2315–2321.

Foreman, M.G.G., D. K. Lee, J. Morrison, S. Macdonald, D. Barnes, and I. V. Williams, 2001: Simulations and retrospective analyses of Fraser watershed flows and temperatures. *Atmos.–Ocean,* **39,** 89–105.

Georgiyevsky, V. Yu., A.V. Yezhov, A.L. Shalygin, A.I. Shiklomanov, and I.A. Shiklomanov, 1996: Evaluation of possible climate change impact on hydrological regime and water resources of the former USSR rivers. *Russ. Meteorol. Hydrol.,* **11,** 89–99.

Glantz, M. H., R. W. Katz, and N. Nicholls, (Eds.), 1991: *Teleconnections Linking Worldwide Climate Anomalies*. Cambridge University Press, New York, 527 pp.

Hamlet, A.F., and D. P. Lettenmaier, 1999: Columbia River streamflow forecasting based on ENSO and PDO climate signals. *ASCE J. Water Res. Plan. Manage.,* **125,** 333–341.

Heredia Calderon, E., and R. Pombosa Loza, 1999: Influencia del ENSO Sobre los Caudales Mensuales de las Grandes Cuencas Hidrograficas del Ecuador, paper presented at Hydrological and Geochemical Processes in Large Scale River Basins Conference, Manaus, Brazil, Amazon Basin Project (HiBAm), University of Brasilia, 15–19 November 1999.

Hurrell, J. W., 1995: Decadal trends in the North Atlantic Oscillation regional temperatures and precipitation. *Science,* **269,** 676–679.

Hurrell, J.W., and H. van Loon, 1997: Decadal variations in climate associated with the North Atlantic Oscillation. *Clim. Change,* **36,** 301–326.

Klein, S. A., B. J. Soden, and N.-C. Lau, 1999: Remote sea surface temperature variations during ENSO: Evidence for a tropical atmospheric bridge. *J. Clim.,* **12,** 917–932.

Krasovskaia, I., 1995: Quantification of the stability of river flow regimes. *Hydrol. Sci. J.,* **40,** 587–598.

Kundzewicz, Z.W., and K. Takeuchi, 1999: Flood protection and management—Quo vadimus? *Hydrol. Sci. J.,* **44** (3), 417–432.

Ludwig, W., and J.-L. Probst, 1998: River sediment discharge to the oceans: Present-day controls and global budgets. *Am. J. Sci.,* **298,** 265–295.

Magnuson, J. J., et al., 2000: Historical trends in lake and river ice cover in the Northern Hemisphere. *Science,* **289,** 1743–1746.

Marengo, J.A., 1999: Interdecadal and long-term variability of the hydrometeorology of the Brazilian Amazon Basin, paper presented at Hydrological and Geochemical Processes in Large Scale River Basins Conference, Manaus, Brazil, Amazon Basin Project (HiBAm), University of Brasilia, 15–19 November 1999.

McCabe, G. J., and M. D. Dettinger, 1999: Decadal variations in the strength of ENSO teleconnections with precipitation in the western United States. *Int. J. Climatol.,* **19,** 1399–1410.

Milly, P. C. D., and K. A. Dunne, 1998: Non-detectability of twentieth-century trends in river discharge from large basins—Observational and model-based results. Preprints, *Ninth Symp. on Global Change Studies and Namias Symp. on the Status and Prospects for Climate Prediction,* Phoenix, AZ, Amer. Meteor. Soc., 162–163.

Molinier, M., J. L. Guyot, G. Cochonneau, V. S. Guimaraes, and E. Oliveira, 1999: La Variabilite Hydrologique du Bassin Amazonien et la Circulation Atmospherique Oceanique, paper presented at Hydrological and Geochemical Processes in Large Scale River Basins Conference, Manaus, Brazil, Amazon Basin Project (HiBAm), University of Brasilia, 15–19 November 1999.

New, M., M. Hulme, and P. Jones, 2000: Representing twentieth-century space–time climate variability. Part II: Development of 1901–96 monthly grids of terrestrial surface climate. *J. Clim.,* **13,** 2217–2238.

Ordoñez Galvez, J.J., 1999: Analisis y Tendencia de los Años de El Niño en la Cuenca Amazonica Peruana, paper presented at Hydrological and Geochemical Processes in Large Scale River Basins Conference, Manaus, Brazil, Amazon Basin Project (HiBAm), University of Brasilia, 15–19 November 1999.

Piovano, E.L., P.J. Depetris, and J. L. Probst, 1999: The hydrological signal of ENSO in the upper Parana drainage basin, paper presented at Hydrological and Geochemical Processes in Large Scale River Basins Conference, Manaus, Brazil, Amazon Basin Project (HiBAm), University of Brasilia, 15–19 November 1999.

Potter, C. S., and S. A. Klooster, 1999: Detecting a terrestrial biosphere sink for carbon dioxide: Interannual ecosystem modeling for the mid-1980s. *Clim. Change,* **42** (3), 489–503.

Potter, C. S., S. Klooster, C. R. de Carvalho, V. Brooks-Genovese, A. Torregrosa, J. Dungan, M. Bobo, and J. Coughlan, 2001: Modeling seasonal and interannual variability in ecosystem carbon cycling for the Brazilian Amazon region. *J. Geophys. Res.,* **106,** 10,423–10,446.

Potter, C., S. Klooster, M. Steinbach, P. Tan, V. Kumar, S. Shekhar, R. Nemani, and R. Myneni, 2003: Global teleconnections of climate to terrestrial carbon flux. *J. Geophys. Res.,* **108,** 4556, doi:10.1029/2002JD002979.

Ramankutty, N., and J. Foley, 1999: Estimating historical changes in global land cover: Croplands from 1700 to 1992. *Global Biogeochem. Cycles,* **13,** 997–1027.

Robertson, A. W., C. R. Mechoso, and N. O. Garcia, 2001: Interannual prediction of the Parana river. *Geophys. Res. Lett.,* **22,** 4235–4238.

Ronchail, J., 1999: Weakness of the relationship between rainfall and ENSO in the lowlands of Bolivia, paper presented at Hydrological and Geochemical Processes in Large Scale River Basins Conference, Manaus, Brazil, Amazon Basin Project (HiBAm), University of Brasilia, 15–19 November 1999.

Serreze, M.C., J. E. Walsh, F. S. Chapin III, T. Osterkamp, M. B. Dyurgerov, V. Romanovsky, W. C. Oechsel, J. Morrison, T. Zhang, and R. G. Barry, 2000: Observational evidence of recent change in the northern high-latitude environment. *Clim. Change,* **46,** 159–207.

Shiklomanov, A.I., 1994: The influence of anthropogenic changes in global climate on the Yenisey River runoff. *Russ. Meteorol. Hydrol.,* **2,** 84–93.

Simpson, H., M. Cane, A. Herczeg, S. Zebiak, and J. Simpson, 1993: Annual river discharge in southeastern Australia related to El Niño–Southern Oscillation forecasts of sea surface temperatures. *Water Resour. Res.,* **29,** 3671–3680.

Sircoulon, J., 1990: Impact possible des changements climatiques à venir sur les ressources en eau des régions arides et semi-arides. Comportement des Cours d'eau Tropicaux, des Rivières et des Lacs en Zone Sahèlienne, World Climate Action Programme 12, *WMO Tech. Doc. 380,* World Meteorological Organisation, Geneva, Switzerland.

Thornthwaite, C. W., 1948: An approach toward rational classification of climate. *Geogr. Rev.,* **38,** 55–94.

Trenberth, J. W., and K. E. Hurrell, 1994: Decadal atmosphere–ocean variations in the Pacific. *Clim. Dyn.,* **9,** 303–319.

Vörösmarty, C.J., and D. Sahagian, 2000: Anthropogenic disturbance of the terrestrial water cycle. *BioScience,* **50,** 753–765.

Vörösmarty, C.J., B. Fekete, and B.A. Tucker, 1998: River Discharge Database, version 1.1 (RivDIS v1.0 supplement). Institute for the Study of Earth, Oceans, and Space, University of New Hampshire, Durham, NH. [Available online at http://www.rivdis.sr.unh.edu/unesco/vol0Overview.html.]

Vörösmarty, C.J., B.M. Fekete, M. Meybeck, and R. Lammers, 2000: A simulated topological network representing the global system of rivers at 30-minute spatial resolution (STN-30). *Global Biogeochem. Cycles,* **14,** 599–621.

Vuille, M., R. S. Bradley, and F. Keimig, 2000: Climate variability in the Andes of Ecuador

and its relation to tropical Pacific and Atlantic sea surface temperature anomalies. *J. Clim.,* **13,** 2520–2535.

Walker, G. T., and E. W. Bliss, 1932: World Weather V. *Mem. Roy. Meteorol. Soc.,* **4,** 53–84.

Whetton, P., D. Adamson, and M. Williams, 1988: Rainfall and river flow variability in Africa, Australia and east Asia linked to El Niño–Southern Oscillation events. *Geolog. Soc. Aust. Symp. Proc.,* **1,** 71–82.

Yang, D., D. Kane, L. Hinzman, X. Zhang, T. Zhang, and H. Ye, 2002: Siberian Lena River hydrologic regime and recent change. *J. Geophys. Res.,* **107,** 4694, doi:10.1029/2002JD002542.